

DOI: 10.37943/ACWT2121

B. Imankulova

Ph.D. Doctoral student of CS
b.imankulova@edu.iitu.kz, orcid.org/0000-0002-6488-6950
International Information Technology University, Kazakhstan

S. Alpar

Ph.D. Doctoral student
s.alpar@iitu.edu.kz, orcid.org/0000-0003-0579-4180
International Information Technology University, Kazakhstan

S. Amanzholova

Candidate of tech. sciences, Assistant professor of department
Cybersecurity
s.amanzholova@edu.iitu.kz, orcid.org/0000-0002-6779-9393
International Information Technology University, Kazakhstan

DATA SECURITY, MODELING AND VISUALIZATION OF DATA FROM IOT DEVICES

Abstract. The article describes the IoT infrastructure, the hardware of the IoT system, considers the issue of security of the chosen LoRa data transmission technology. Data was received from sensors for gas, temperature and humidity, atmospheric pressure, as well as the location of the end device. At the same time, the standardized security features of the selected LoRa technology for transmitting data from sensors to the server were investigated. The article deals with LoRa bi-directional secure communication line, the security function requires devices/end devices to be configured through the LoRa gateway. Security research is devoted to the development of a security mechanism to increase its resilience. The payload was formed with a hash of the last bytes, and the entire payload was encrypted with AES for integrity and confidentiality. A method for assessing and visualizing atmospheric air pollution is given on the example of the city of Almaty, Kazakhstan. The process of numerical modeling of the study of emissions of harmful substances into the atmosphere is based on a mathematical model formed by the system of Navier-Stokes equations, consisting of the continuity equation, as well as the equations of motion and the k-epsilon turbulence model. To test the numerical methods for processing mixing and chemical reactions, a test problem was chosen – a jet in a transverse flow. Three-dimensional numerical simulation has been implemented. The use of the Internet of Things (IoT) and the acquisition of big data made it possible to simultaneously observe the concentrations of several pollutants in the atmosphere, calculate this concentration and analyze the state of the surface air layer. Modeling allows forecasting the possible concentration of pollutants in certain areas at certain times of the year.

Key words: IoT framework, sensors, monitoring, computer modeling, data collection, data processing, big data, data systematization, LoRa, security, AES.

Introduction

Today, the Internet of Things (IoT) is a relevant topic for study. IoT development supports a variety of applications, IoT sensors allow monitoring air temperature and humidity, atmospheric pressure, air quality and they are scalable, have online updates, solving air monitoring issues

efficiently. The functions of IoT are real-time data collection, and its further processing and data analysis allow the assessment of urban air pollution.

The environmental monitoring system was deployed based on the LoRa (Long Range) [1], which was tested in several locations in Almaty. The selected data transmission technology LoRa is a low-power wireless network (WAN) communication technology, which has several advantages in IoT applications. LoRa technology uses Spread Spectrum Modulation (SSM) and Chirp Spread Spectrum (CSS) variations with integrated Forward Error Correction (FEC), thereby transmitting signals over a large bandwidth, providing a large range [2]. The LoRa network was built according to the “star” topology [3], which is determined by the physical layer. The advantage of using this topology is to extend the battery life and offload the network, where nodes do not need to receive and forward data from other nodes. Based on the comparison presented in [4, 5], within the framework of this project, LoRaWAN technology was chosen as the most suitable for data transmission over long distances with low energy consumption.

In work [6], the authors obtained and processed the data for the first time, they gave the solutions of the semi-empirical equation of turbulent diffusion, and a comprehensive calculation of the Air Quality Index (AQI) was determined. In work [7], a study of the impact of pollution on the environment and the human body was carried out, calculations were made, and recommendations were given. The paper [8] describes the analysis of big data, and a zoning map of the city of Almaty was also built based on the data and the points of pollution were indicated.

This article presents an environmental monitoring system, this system is modular in terms of hardware and software. While constructing the system, such aspects as energy consumption of equipment, reliability and its cost were taken into account.

Hardware implementation

The system consists of the following devices: ATmega2560 microcontroller, LoRa Shield based on module SX1276/SX1278 is a long range transceiver operating at 868 MHz (fig.1). Temperature and humidity, atmospheric pressure, gas sensor, real-time sensor, GPS, SD card and 4000 mAh battery were combined into end devices (or Nodes) that transmit payload data to the LoRa gateway in an uplink message. When a data is received from Nodes, the gateway forwards it to The Things Network (TTN) server [9] as a hexadecimal code. The terminal unit is enclosed in a sealed plastic case, which provides protection against dust and water.

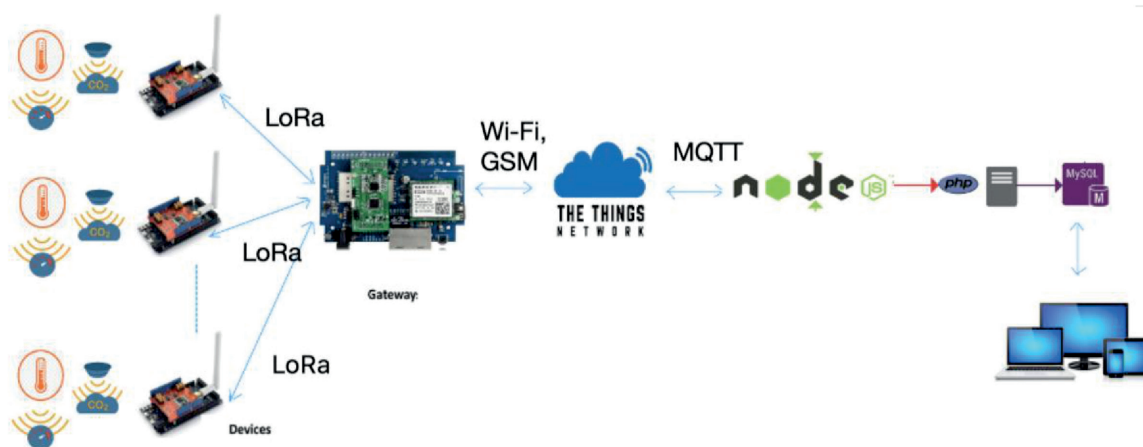


Figure 1. Architecture of the environmental monitoring system

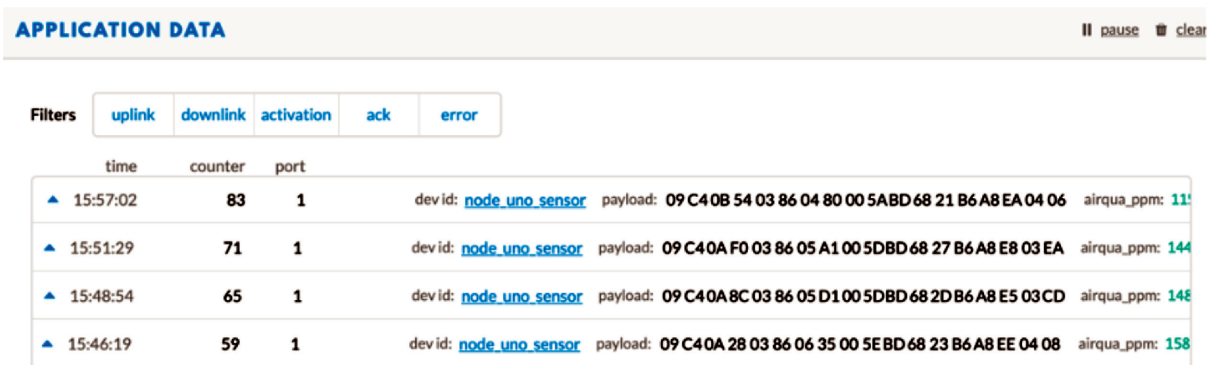
The software of the environmental monitoring system was created on the NodeJS platform, which stores data using a MySQL database. The server is responsible for receiving, transmitting, storing and displaying the data from the nodes. The received data from the network server

is written to the MySQL database using the database storage table field. The data is then analyzed, thus performing visualization and readability of the monitoring data.

LoRa and security aspects

The main parameters of the LoRa device that need to be configured are the spreading factor (SF), it ranges from 7 to 12 (in our case it was set to 7), the coding rate (CR) - the value varies from 4/5 to 4/8 and bandwidth (BW) - 125, 250 or 500 kHz. As mentioned earlier, the operating frequency of the module is 868 MHz, the allocated bandwidth is 125 kHz.

From the end node to the gateway, the data comes in the form of a hexadecimal code (HEX) string of 18 bytes in size, which contains readings from all sensors of one node at one point in time. An example of the received data lines is shown in fig. 2.



APPLICATION DATA							pause	clear			
Filters							uplink	downlink	activation	ack	error
	time	counter	port	dev id:	payload:	airqua_ppm:					
▲	15:57:02	83	1	node_uno_sensor	09 C40B 54 03 86 04 80 00 5ABD 68 21 B6 A8 EA 04 06	111					
▲	15:51:29	71	1	node_uno_sensor	09 C40A F0 03 86 05 A1 00 5DBD 68 27 B6 A8 E8 03 EA	144					
▲	15:48:54	65	1	node_uno_sensor	09 C40A 8C 03 86 05 D1 00 5DBD 68 2D B6 A8 E5 03 CD	148					
▲	15:46:19	59	1	node_uno_sensor	09 C40A 28 03 86 06 35 00 5EBD 68 23 B6 A8 EE 04 08	158					

Figure 2. TTN payload

Paying attention to the issue of security, we need to study the issue of the security of the gateway or IP devices on the Internet. At the same time, it is necessary to pay attention to the issue of security between the gateway and end devices. This section describes how to establish a secure connection between the LoRa gateway and IoT end devices. Fig.3 shows the block diagram of the system.

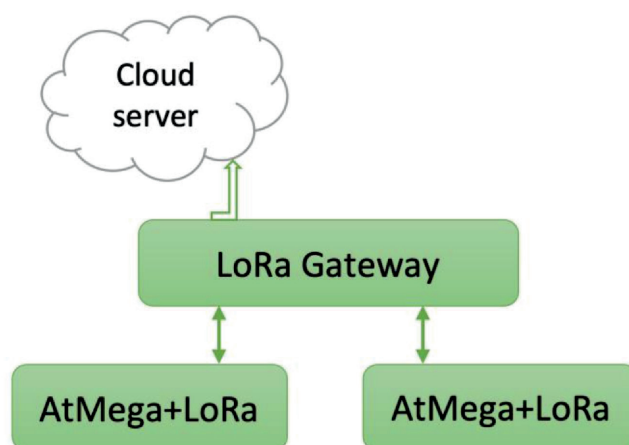


Figure 3. System block diagram

The software architecture consists of some parts, i.e. layers, such as the server layer (SDK). This also includes the client part, drivers, LoRa libraries. Framework C++ is the next level (in many cases there may not be a framework due to the limited resources of the microcontroller). The last level is the implementation of the application for the client.

Secure link. A secure connection has been established, headers have been added for the uplink and downlink messages (where the message commands are defined, e.g. join request, answer, join type, etc.), followed by the Payload and finally the message integrity code is checked (MIC).

If we follow the classic definition of security, we have to think about channel confidentiality, integrity and authenticity, and system availability. The LoRa module supports 128-bit AES data encryption. Using the Advanced Encryption Standard (AES), the data sent from the IoT devices to the gateway will be encrypted and LoRa uses three different keys, such as Application key, Network session key, and Application session key. The Network session key protects the network infrastructure and the server, also the end-to-end connection is protected by the Application session key. Keys can be monitored using two activation methods: Activation By Personalization (ABP) and Over The Air Activation (OTAA). Noted [10] that devices using pre-shared keys for encryption and decryption, i. in the ABP model, vulnerable to attacks. However, pre-shared secret keys can also be captured by node takeover attacks. OTAA is the preferred activation method, as it provides the most secure way to connect end devices to a network server before activation [9]. Dev EUIs are already in the devices. Dev EUI stands for 64-bit Extended Unique Identifier, which is commonly used to identify network components. Dev EUI is similar to the MAC address of the device and identifies the end device.

The Cryptographic Message Integrity Code (MIC) is used in LoRa to provide integrity checking of the MAC header and payload data. After the session key is generated, the MIC is calculated in CMAC mode. As for the function of the counter, it is also an important component of the protection of the communication channel, since the message counter is used to generate the keystream, that is, there are two frame counters on the uplink and downlink on the network server for each end device. Counters overflow over time and there may be repetitions of the count, which can lead to vulnerabilities. End devices must be physically protected (have non-volatile memory as an example) to prevent a system reset from being triggered. In an IoT context, this part can be difficult to complete, depending on the difference in deployment.

Payload. Before calculating the message integrity code, the payload can be encrypted at the application layer.

Modelling and experimental results

Simulation settings. The simulations were performed in the ANSYS Workbench environment, namely the calculations were performed in the ANSYS Fluent software package, and the parametric geometry model was built in ANSYS Geometry.

To test the numerical methods in the processing of mixing and chemical reactions, a test problem was chosen jet in the cross-flow situation. Fig. 4 shows the directions and dimensions of the calculated area, where substance A passes through the left edge of "in1", substance B enters through the input of the tube "in2", "out" - the output, through the right edge. Grid size of the main channel is 641x161 elements, grid size of the tube at the second input is 41x81 elements. The entire computational area contains 106,481 nodes, 211,200 elements, 638,886 unknown quantities (the dimensions of the physical area are given in meters). The laminar viscosity method is used to solve the system of Navier-Stokes equations for an incompressible fluid in ANSYS Fluent. The mass fraction of the substance was calculated using Species Transport. The SIMPLE method was used for the numerical discretization of equations, and $\varepsilon = 0.00001$ was taken as the convergence condition.

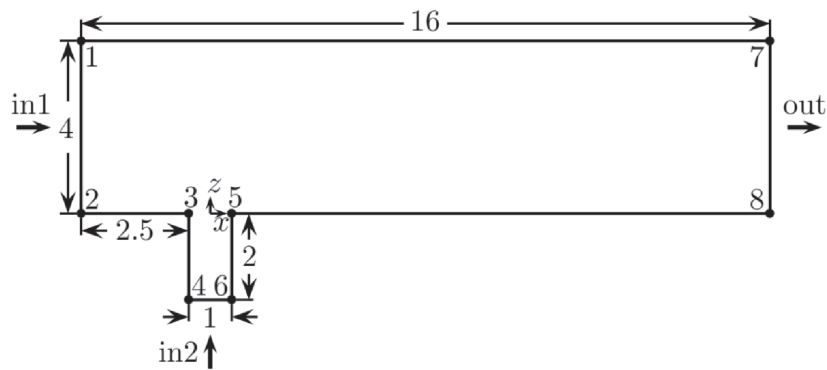


Figure 4. Diagram of the computational domain for a cross-flow jet Velocity ratios

$$R = \frac{U_{jet}}{U_{crossflow}} = 1.5$$

Where, U_{jet} is the average velocity in the pipe,
 $U_{crossflow}$ is reference velocity far from the wall.

Small Mach number guarantees us noncompressible state. A similar study was conducted by foreign researchers [11-15], and the purpose of this study was to compare and validate the numerical methods with the results obtained by the authors.

Mathematical model. The numerical modeling process for the study of emissions of harmful substances into the atmosphere is based on a mathematical model formed by the system of Navier-Stokes equations, consisting of the continuity equation, as well as the equations of motion and the k-epsilon model of turbulence.

$$\frac{\partial u_j}{\partial x_j} = 0 \quad (1)$$

$$\frac{\partial p u_j}{\partial t} + \frac{\partial}{\partial x_j} (p u_i u_j) = -\frac{\partial p'}{\partial x_i} + \frac{\partial}{\partial x_j} \left[\mu_{eff} \left(\frac{\partial u_i}{\partial x_j} + \frac{\partial u_j}{\partial x_i} \right) \right] \quad (2)$$

where p' – pressure, μ_{eff} – effective viscosity.

$$\frac{\partial k}{\partial t} + \frac{\partial}{\partial x_j} (u_j k) = \frac{\partial}{\partial x_j} \left[\left(\mu + \frac{\mu_t}{\sigma_k} \right) \frac{\partial k}{\partial x_j} \right] + P_k - \rho \varepsilon + P_{kb} \quad (3)$$

$$\frac{\partial \varepsilon}{\partial t} + \frac{\partial}{\partial x_j} (u_j \varepsilon) = \frac{\partial}{\partial x_j} \left[\left(\mu + \frac{\mu_t}{\sigma_\varepsilon} \right) \frac{\partial \varepsilon}{\partial x_j} \right] + \frac{\varepsilon}{k} (C_{\varepsilon 1} P_k - C_{\varepsilon 2} \rho \varepsilon + C_{\varepsilon 1} P_{\varepsilon b}) \quad (4)$$

P_k – the product of turbulence, obtained due to viscous forces, which is presented in the form as:

$$P_{\varepsilon b} = C_3 \max(0, P_{kb}) \quad (5)$$

$C_{\varepsilon 1}, C_{\varepsilon 2}, \sigma_k, \sigma_\varepsilon$ – are constants: $C_{\varepsilon 1} = 1,45, C_{\varepsilon 2} = 1,9, \sigma_k = 1,0, \sigma_\varepsilon = 1,3$, dissipation coefficient $C_3=1$

Matter transfer equations. In order to solve the equations of matter transfer, the ANSYS Fluent software package calculates the local mass fraction of each Y_i substance by solving the convection-diffusion equation for the i -th kind.

$$\frac{\partial}{\partial t} (\rho Y_i) + \nabla (\rho \vec{u} Y_i) = -\nabla \cdot \vec{J}_i + R_i + S_i \quad (6)$$

Here R_i is the net rate of formation of a substance i by chemical reaction and S_i rate of formation by addition from the dispersed phase plus any user-defined sources. The equation

of this form will be solved for $N-1$ particles, where N is the total number of chemical particles in the liquid phase that are considered in the given system. Since the total mass fraction of particles must be equal to one, then the mass fraction N will be determined as one minus the sum of the solved mass fractions $N-1$.

It is worth mentioning that for turbulent flows, the mass diffusion will be calculated as:

$$\vec{J}_i = -\left(\rho D_{i,m} + \frac{\mu_t}{Sct}\right) \nabla Y_i \quad (7)$$

Where $Sct = \frac{\mu_t}{\rho D_t}$ – turbulent Schmidt number (μ_t – turbulent viscosity and D_t – turbulent diffusivity). The default Sct is 0,7. In this research it was set as 1.

Energy equation.

$$\frac{\partial}{\partial t}(\rho E) + \nabla(\vec{v}(\rho E + p)) = \nabla \cdot \left(k_{eff} \nabla T - \sum_j h_j \vec{J}_j + (\vec{\tau}_{eff} \cdot \vec{v})\right) + S_h \quad (8)$$

Here $k_{eff} = k + k_t$ – effective conductivity, where k_t – turbulent thermal conductivity, determined according to the turbulence model, J_j – is the diffusion flux of components j . The first 3 components on the RHS of (12) express energy transfer due to conduction, species diffusion, and viscous dissipation, respectively. S_h – take into account the energy of chemical reaction.

Boundary conditions. For the input of the main channel (In1), different variants of the velocity profile were considered (this parameters given in the table 1):

$$u1: u = u^* \quad (9)$$

$$u2: u = u^* \left(1 - e^{-4,5\left(1 - \frac{r^2}{4}\right)}\right), r = y \quad (10)$$

$$u3: u = u^* \left(1 - e^{-5\left(1 - \frac{r^2}{4}\right)}\right), r = y \quad (11)$$

$$u4: u = u^* \left(1 - e^{-5,5\left(1 - \frac{r^2}{4}\right)}\right), r = y \quad (12)$$

Other parameters are taken as: $w = 0$, $Y_A = 1$, $Y_B = 1$.

For pipe entry In2:

$$u=0, w=2Ru^*(1-4l^2), l=x, Y_A = 0, Y_B = 0 \quad (13)$$

Here u^* varies depending on the selected material. Oxygen O_2 was taken for substance A and B. In order to derive the Reynolds number ($Re = \rho u_{crossflow} D / \mu = 25$), the fact that the dynamic viscosity of oxygen is equal to $\mu = 1,919e-05$ kgm²/s, density to $\rho = 1,299874$ kg/m³, velocity to $u^* = 0,000369074233$ m/s, and the hydraulic diameter is equal to $D=1$ m is taken into account. In order for the Schmidt number to be equal to one, the diffusion coefficient is defined as a number that equal to 0,67737051 m²/s.

In the ANSYS Fluent software package, all calculations are performed in real physical dimensions. The ANSYS Fluent sampling method uses the test volume method (FVM).

Table 1. The main parameters of the boundary conditions

Parameters	In1	In2	Wall	Out
u	See (9) – (12)	$u = 0$	$u = 0$	$\frac{\partial u}{\partial x} = 0$
w	$w = 0$	See (18)	$w = 0$	$\frac{\partial w}{\partial x} = 0$
p	See (11)	$p = \text{patmosphere}$	See (11)	See (11)
Y_A	$Y_A = 1$	$Y_A = 0$	$\frac{\partial Y_A}{\partial x} = 0$	$\frac{\partial Y_A}{\partial x} = 0$
Y_B	$Y_B = 1$	$Y_B = 1$	$\frac{\partial Y_B}{\partial x} = 0$	$\frac{\partial Y_B}{\partial x} = 0$
Y_C	$Y_C = 1$	$Y_C = 0$	$\frac{\partial Y_C}{\partial x} = 0$	$\frac{\partial Y_C}{\partial x} = 0$

Testing and visualization

The results of calculations and comparative analysis of the following parameters: velocity and mass fraction of a substance are given below.

Velocity. Fig. 5 shows the results for horizontal and vertical velocity profiles, with an initial velocity profile u_3 in the main channel. It is worth mentioning that it is necessary to establish the velocity profile through a function, and not through a constant, since this will significantly affect the result, allowing a more accurate description of physical processes that give the result as close as possible to real processes.

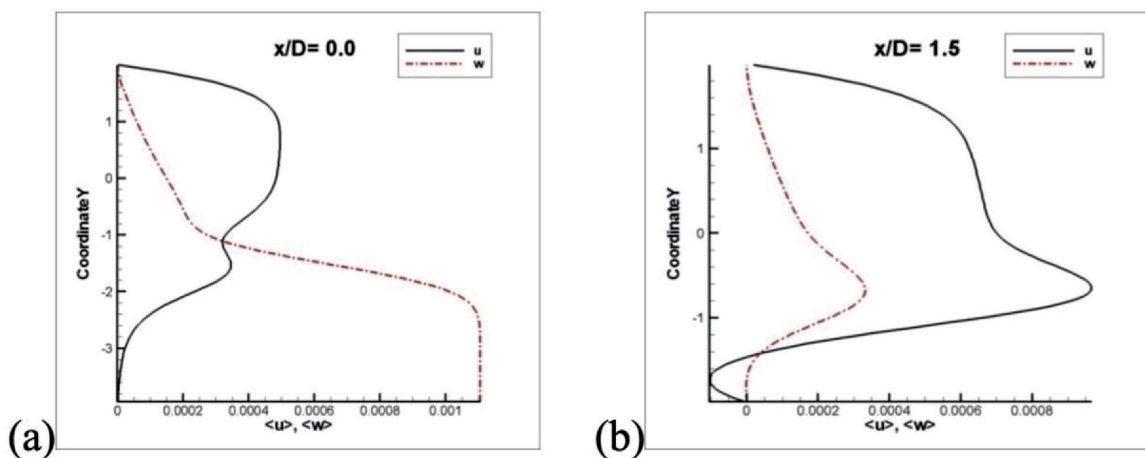


Figure 5. Profiles of the vertical and horizontal velocity components: (a) $x / D = 0,0$, (b) $x / D = 1,5$

Mass fraction. Figures 6, 7 and 8 show the results of the profile of the mass fraction of substances A, B and the resulting reagent C at different sites, respectively. They also clearly show that the difference between the velocity profile and other profiles also affects the particle mass fraction distribution.

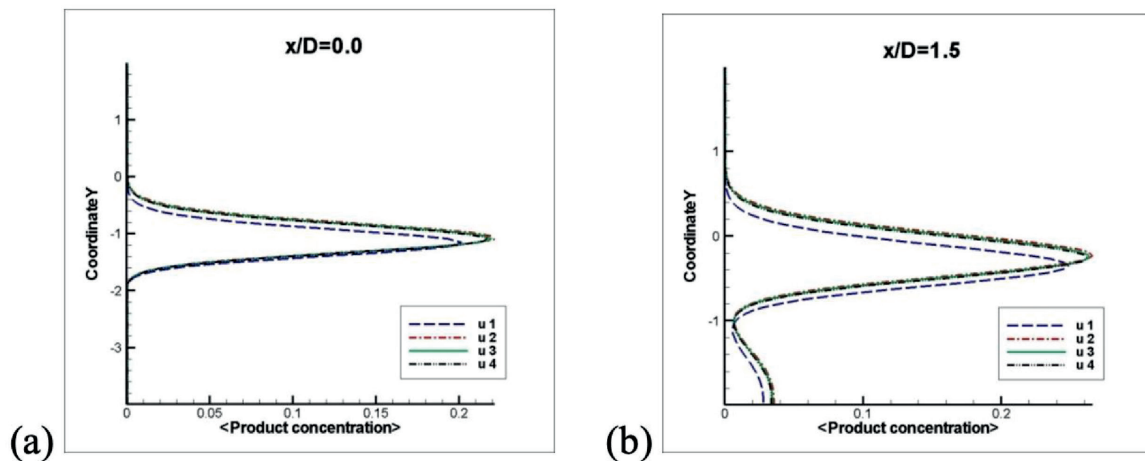


Figure 6. Profiles of the mass fraction of the reaction product C at different distances for different profiles of the initial velocity: (a) $x / D = 0,0$, (b) $x / D = 1,5$

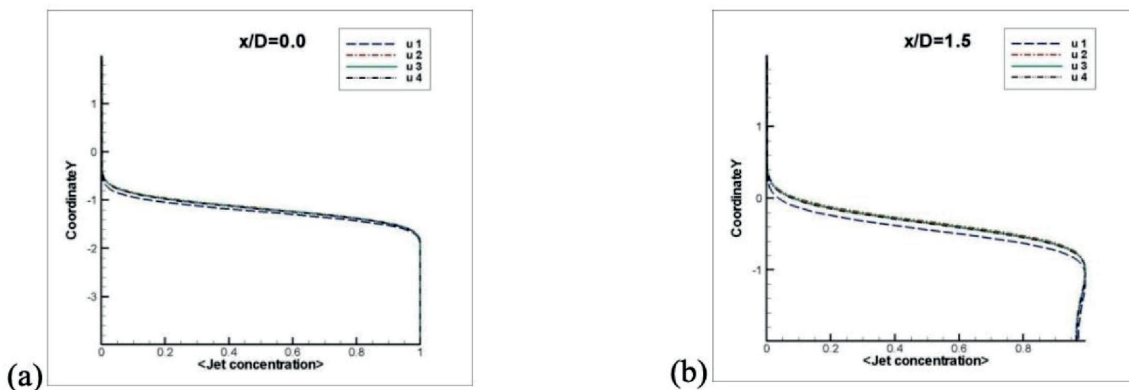


Figure 7. Profiles of the mass fraction of substance B at different distances for different profiles of the initial velocity: (a) $x / D = 0,0$, (b) $x / D = 1,5$

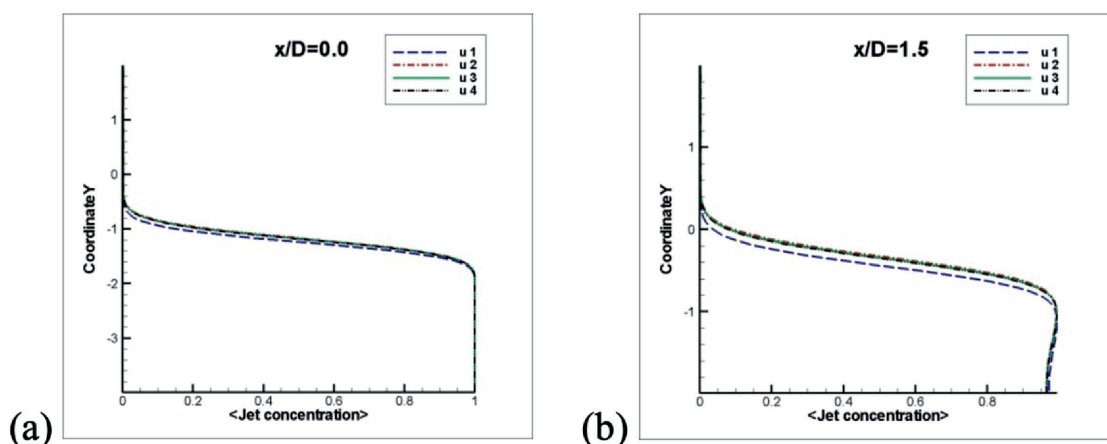


Figure 8. Profiles of the mass fraction of substance A at different distances for different initial velocity profiles: (a) $x / D = 0,0$, (b) $x / D = 1,5$

Figures 9-10 show a comparative analysis of the scatter of mass fractions obtained in the course of this work and the results of foreign researchers [12, 13, 15], where C_1 , C_2 , C_3 are the mass fractions of substances A, B and C, respectively.

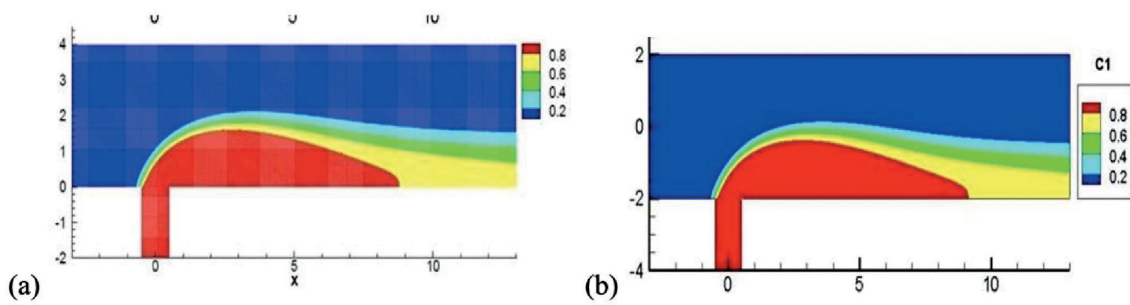


Figure 9. Comparative analysis of the distribution of substance A:
(A) J.A. Denev's results; (B) Results from ANSYS Fluent

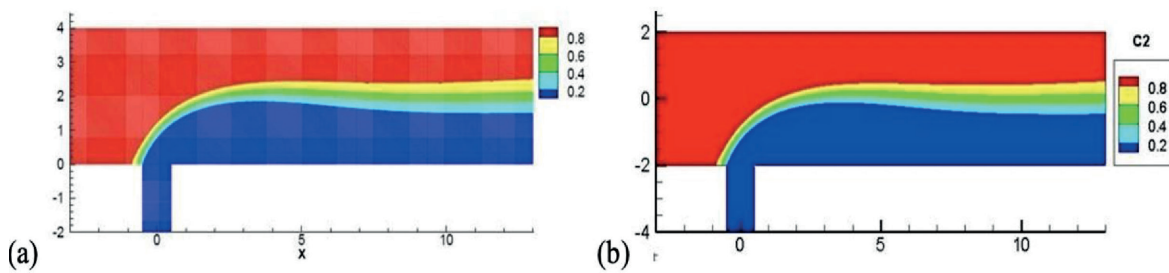


Figure 10. Comparative analysis of the distribution of substance B:
(A) J.A. Denev's results; (B) Results from ANSYS Fluent

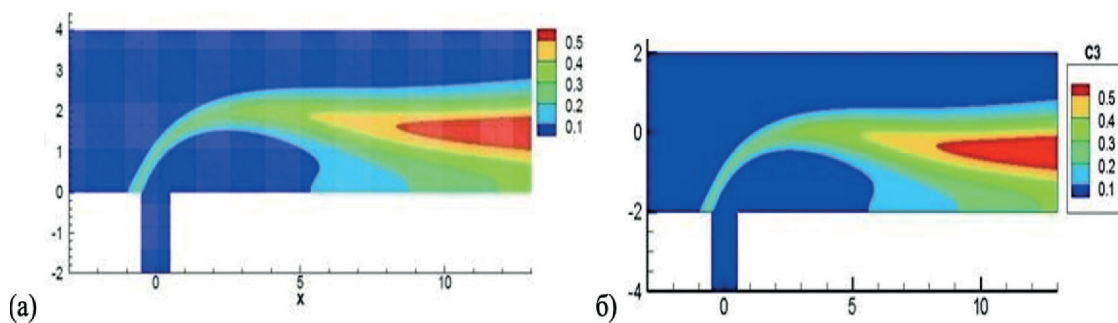


Figure 11. Comparative analysis of the distribution of substance C:
(A) J.A. Denev's results; (B) Results from ANSYS Fluent

From the comparison results, the conclusion that the mathematical model chosen in this study is correct can be made, and it is possible to move on to more complex cases.

Consider a two-dimensional case of the spread of pollution emissions into the atmosphere. A substance was chosen as a pollutant – methane, the wind speed is 0.5 m/s, the pollution speed is 14 m/s. In this case, the effect of the temperature gradient on the level of concentration of the substance was investigated. The temperature gradient is taken with a difference of 5°C: from 22°C to 25°C. The calculations were carried out with a temperature gradient as well as a constant temperature. In addition, the temperature of the pollutant was set at 27°C (Figure 12).

After solving the test problem in a two-dimensional domain, this section deals with a three-dimensional case of this problem. In this version, the area in the form of a parallelepiped with a pipe was chosen as the computational domain. Emissions spread from the pipe opening, and one of the walls was chosen as the entrance for the wind flow. Whereas the opposite wall was identified as an exit. Figure 13 illustrates the geometry and mesh of the computational field with one tube. Many parameters are taken from previous studies by foreign authors [16].

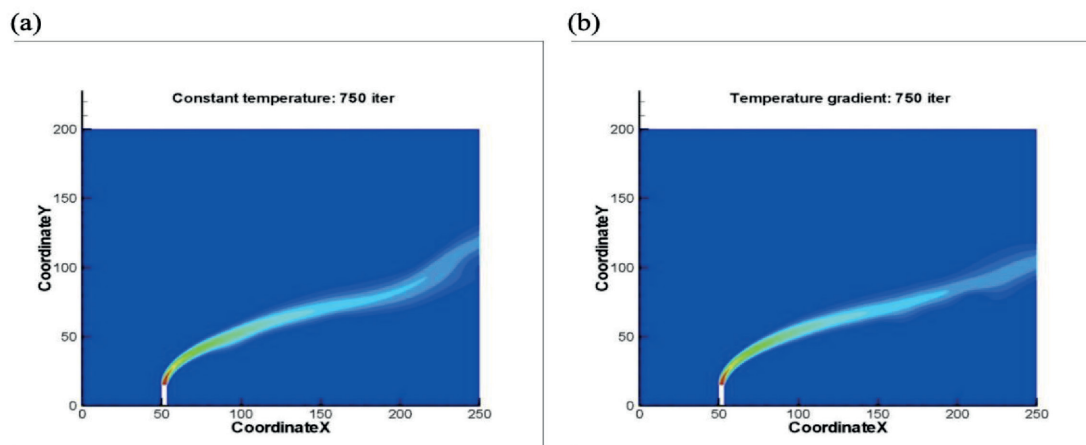


Figure 12. Comparison of the distribution of pollutants due to temperature
(a) constant temperature (b) temperature gradient

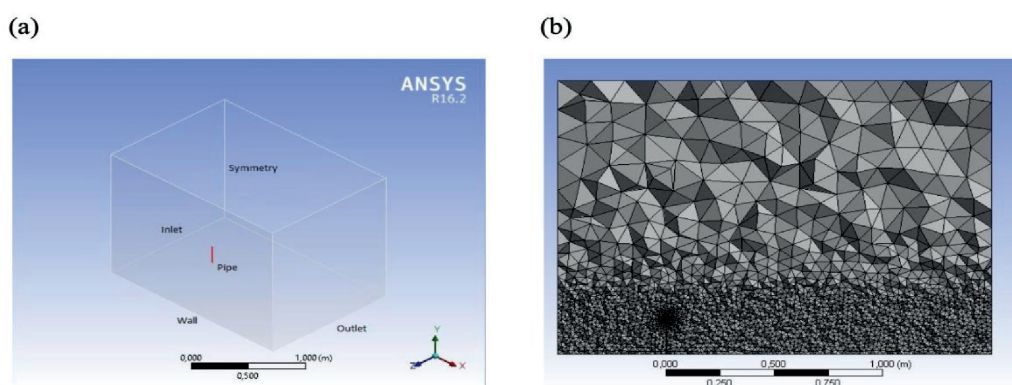


Figure 13. (a) Geometry of the computational domain; (b) Grid

Conclusion

The purpose of this work was to build an IoT framework with secure data transmission, obtaining and studying the received data, analyzing the distribution of emissions of harmful substances in the atmosphere under the influence of air speed, density of the emitted material, pipe dimensions and other atmospheric conditions.

The solution of a simplified model test problem allows to check the correctness of the selected mathematical model and the method of numerical solution, which, in turn, can later be used in the calculations of more complex physical objects and turbulent models.

From the built system, real data was obtained generated by sensors, such as: an air quality measurement sensor, a temperature and humidity sensor, an atmospheric pressure sensor, a real-time sensor and GPS for further processing. Further, these data were used for data analytics for making operational decisions and visualization of basic information for studying air pollution in the city of Almaty and the region. The choice of a network server allowed us to consider security issues in detail. In the article, we introduced standardized LoRa security features, link privacy, integrity and authenticity verification, system availability.

At the beginning of the study, the two-dimensional propagation of matter coming from the jet, which flowed across the main flow, was considered. Physical parameters such as density, dynamic viscosity, hydraulic diameter and velocity were chosen to obtain a fairly low Reynolds number for laminar flow. The results obtained in the work showed that the change in the degree of the exponent as a function of the velocity profile has a significantly significant

effect on the flow of matter but setting the velocity as a constant gives a large error in the calculations. In addition, the analysis showed that the air flow rate significantly affects the nature of movement and the range of distribution of substances.

After obtaining a solution to the two-dimensional problem, three-dimensional numerical modeling was implemented. This study provides a preliminary estimate of the spread of harmful substances in the atmosphere considering physical, climatic and meteorological factors. The constructed condensed computational grid made it possible to minimize computational costs and concentrate all resources on the areas of particular interest. Plus, the movement of the distribution of matter through obstacles was considered. The results show that the height of the pipes significantly influenced the spread of contamination. From this the conclusion that to preserve the ecology, it is necessary to build higher pipes can be made. Also, this research method allows to determine the distance of the spread of harmful substances in the air, which will help to simulate in advance the optimal location of pipes in relation to settlements. It minimizes the damage caused by emissions to humans, flora, and fauna.

Software for modeling air pollution was developed, a spatial database for the study area was created. A proprietary software has been created for modeling air pollution in the form of a software prototype, which provides the ability to simulate in real time, the simulation results are visualized and can be used by researchers for further research.

Future work

It is planned to refine the framework in terms of the dashboard, and in terms of security, there is a need to improve or update the methods used. Sensors can be replaced with industrial types, which will allow the use of improved performance.

References

1. LoRa Alliance Homepage, <https://lora-alliance.org>, last accessed 2022/02/5.
2. LoRa Semtech Homepage, <https://www.semtech.com/lora>, last accessed 2022/03/1.
3. Bankov, D., Khorov, E., Lyakhov, A. (2016) 'On the Limits of LoRaWAN Channel Access'. *Conference: International Conference on Engineering and Telecommunication (EnT)*. DOI: 10-14. 10.1109/EnT.2016.011.
4. Pule, M., Yahya A., Chuma, J. (2017) 'Wireless sensor networks: A survey on monitoring water quality'. *Journal of Applied Research and Technology*. V. 15, Issue 6, pp. 562-570
5. Mekki, K., Bajic, E., Chaxel, F., Meyer, F. (2019) 'A comparative study of LPWAN technologies for large-scale IoT deployment'. *ICT Express*. V. 5, Issue 1, pp. 1-7.
6. Duisebekova, K., Kozhamzharova, D., Rakhmetulayeva, S., Umarov, F., Aitimov, M. (2020). Development of an information-analytical system for the analysis and monitoring of climatic and ecological changes in the environment, *Procedia Computer Science*, 170, 578-583. <https://doi.org/10.1016/j.procs.2020.03.128>
7. Myrzakerimova, A., Shaizat, M., Duisebekova, K., Nurmaganbetova, M. (2020). Forecasting risk of diseases in Kazakhstan with using mapping technique based on 9 years statistics. The 11th International Conference on Ambient Systems, Networks and Technologies (ANT) April 6-9, Warsaw, Poland. *Procedia Computer Science*, 170, 75–81. <https://doi.org/10.1016/j.procs.2020.03.010>
8. Imankulova, B., Amanzholova, S., Duisebekova, K. (2020). Software and technical aspects of data collection from end nodes: problems and prospects. *Bulletin of AUPET*. No 4 (51). 164-172. https://doi.org/10.51775/1999-9801_2020_51_4_164
9. The Thing Network (TTN) Homepage, <https://www.thethingsnetwork.org>, last accessed 2022/03/4.
10. Butun, I., Pereira, N., & Gidlund, M. (2018, June). Analysis of LoRaWAN v1. 1 security. In *Proceedings of the 4th ACM MobiHoc Workshop on Experiences with the Design and Implementation of Smart Objects* (pp. 1-6). <https://doi.org/10.1145/3213299.3213304>.

11. Aras, E., Ramachandran, G.S., Lawrence, P., & Hughes, D. (2017, June). Exploring the security vulnerabilities of LoRa. In *2017 3rd IEEE International Conference on Cybernetics (CYBCONF)* (pp. 1-6). IEEE. <https://doi.org/10.1109/cybconf.2017.7985777>
12. Fearn, R., & Weston, R. P. (1974). Vorticity associated with a jet in a cross flow. *AIAA Journal*, *12*(12), 1666-1671. <https://doi.org/10.2514/3.49576>
13. Andreopoulos, J., & Rodi, W. (1984). Experimental investigation of jets in a crossflow. *Journal of Fluid Mechanics*, *138*, 93–127.
14. <https://doi.org/10.1017/s0022112084000057>
15. Zavila, O. (2012) 'Physical Modeling of Gas Pollutant Motion in the Atmosphere', Advances in Modeling of Fluid Dynamics, Dr. Chaoqun Liu (Ed.), InTech. <https://doi.org/10.5772/48405>
16. Denev, J.A., Frohlich, J., & Bockhorn, H. (2007). Direct numerical simulation of a transitional jet in crossflow with mixing and chemical reactions. In *Fifth International Symposium on Turbulence and Shear Flow Phenomena*. Begel House Inc. <https://doi.org/10.1615/tsfp5.1940>
17. Falconi, C., Denev, J., Frohlich, J., & Bockhorn, H. (2007). 'A test case for microreactor flows – a two-dimensional jet in crossflow with chemical reaction', Internal Report. 2d test case for microreactor flows.